

Prediction the Effects of ZnO₂ Nanoparticles on Splitting Tensile Strength and Water Absorption of High Strength Concrete

Ali Nazari*, Tohid Azimzadegan

Department of Materials Science and Engineering, Saveh Branch, Islamic Azad University, Saveh, Iran

Received: September 9, 2010; Revised: April 3, 2012

In the present paper, two models based on artificial neural networks (ANN) and gene expression programming (GEP) for predicting splitting tensile strength and water absorption of concretes containing ZnO₂ nanoparticles at different ages of curing have been developed. To build these models, training and testing using experimental results for 144 specimens produced with 16 different mixture proportions were conducted. The used data in the multilayer feed forward neural networks models and input variables of genetic programming models are arranged in a format of eight input parameters that cover the cement content (C), nanoparticle content (N), aggregate type (AG), water content (W), the amount of superplasticizer (S), the type of curing medium (CM), Age of curing (AC) and number of testing try (NT). According to these input parameters, in the neural networks and genetic programming models, the splitting tensile strength and water absorption values of concretes containing ZnO₂ nanoparticles were predicted. The training and testing results in these two models have shown the strong potential of the models for predicting the splitting tensile strength and water absorption values of concretes containing ZnO₂ nanoparticles. Although neural networks have predicted better results, genetic programming is able to predict reasonable values with a simpler method rather than neural networks.

Keywords: *neural networks, genetic programming, nanoparticles, concrete, tensile test, water permeability*

1. Introduction

Strength assessment of concrete is a main and probably the most important mechanical property, which is usually measured after a standard curing time. Concrete strength is influenced by lots of factors like concrete ingredients, age, ratio of water to cementitious materials, etc. The pore structure determines the transport properties of cement paste, such as permeability and ion migration. Permeability of cement paste is a fundamental property in view of the durability of concrete: it represents the ease with which water or other fluids can move through concrete, thereby transporting aggressive agents. It is therefore of utmost importance to investigate the quantitative relationships between the pore structure and the permeability. Through experimental studies and then numerical simulations of the pore structure and the permeability of cement-based materials, a better understanding of transport phenomena and associated degradation mechanisms will hopefully be reached¹.

Conventional methods of predicting various properties of concrete are generally based on either water to cement ratio rule or maturity concept of concrete². Over the last two decades, a different modeling method based on neural networks (NNs) has become popular and used by many researchers for a wide range of engineering applications. NNs are a family of massively parallel architectures that

solve difficult problems via the cooperation of highly interconnected but simple computing elements (or artificial neurons). Basically, the processing elements of a neural network are analogous to the neurons in the brain, which consist of many simple computational elements arranged in several layers³. The concrete properties could be calculated using the models built with NNs. It is convenient to use these models for numerical experiments to review the effects of each variable on the mix proportions^{4,6}. Besides ANNs, genetic programming (GP) has begun to arise for the explicit formulation of the properties and the performances of concrete recently^{7,8}. Genetic programming offers many advantages as compared to classical regression techniques. Regression techniques are often based on predefined functions where regression analyses of these functions are later performed. On the other hand, in the case of GP approach, there is no predefined function to be considered. In this sense, GP can be accepted to be superior to regression techniques and neural networks. GP has proven to be an effective tool to model and obtain explicit formulations of experimental studies including multivariate parameters where there are no existing analytical models^{7,8}.

In our previous works, the effects of different types of nanoparticles on physical and mechanical aspects of concrete specimens were studied⁹⁻²⁷. The aim of this study is to predict splitting tensile strength and water

*e-mail: alinazari84@aut.ac.ir

absorption of several types of concrete with and without ZnO₂ nanoparticles by ANNs and GP. Totally 144 splitting tensile strength and 144 percentages of water absorption data from 16 different concrete mixtures were collected, trained and tested by means of different models. The obtained results have been compared by experimental ones to evaluate the software power for predicting the properties of concrete.

2. Experimental Procedure

2.1. Materials

Two series of concrete were made in the laboratory. The first was normally vibrated concrete (NVC) series with ordinary river sand as aggregates and the second self compacting concrete (SCC) series with limestone aggregates. The utilized materials are as below:

Ordinary Portland Cement (OPC) conforming to ASTM C150^[28] standard was used as received. The chemical and physical properties of the cement are shown in Table 1.

ZnO₂ nanoparticles with average particle size of 15 nm and 45 m².g⁻¹ Blaine fineness producing from Suzhou Fuer Import & Export Trade Co., Ltd was used as received. The properties of ZnO₂ nanoparticles are shown in Table 2.

Locally available natural sand with particles smaller than 0.5 mm and fineness modulus of 2.25 and specific gravity of 2.58 g.cm⁻³ was used as fine aggregate for NVC series concrete. Crushed basalt stored in the laboratory with maximum size of 15 mm and specific gravity of 2.96 g.cm⁻³ was used as coarse aggregate in NVC series concrete.

Crushed limestone aggregates were used to produce self-compacting concretes, with gravel 4/12 and two types of sand: one coarse 0/4, for fine aggregates and the other fine 0/2, with a very high fines content (particle size < 0.063 mm) of 19.2%, the main function of which was to provide a greater volume of fine materials to improve the stability of the fresh concrete. A polycarboxylate with a polyethylene condensate defoamed based admixture (Glenium C303 SCC) was used. Table 3 shows some of the physical and chemical properties of polycarboxylate admixture used in this study.

2.2. Mixture proportions

Totally 6 series of mixtures were prepared and tested experimentally. C0 series mixtures were prepared as control specimens. The control mixtures were made of natural aggregates, cement and water. C0 series mixtures were cured in water (W) and saturated limewater (LW) and designated as C0-W and C0-LW series, respectively. N series were prepared with different contents of ZnO₂ nanoparticles. The mixtures were prepared by the cement replacement of 0.5, 1.0, 1.5 and 2.0 weight percent. N series mixtures were

also cured in water (W) and saturated limewater (LW) and designated as N-W and N-LW series, respectively.

C0-SCC series mixtures were prepared by cement, fine and ultra-fine crushed limestone aggregates with 19.2% by weight of ultra-fine ones and 1.0 weight percent of polycarboxylate admixture replaced by water. N-SCC series were prepared with different contents of ZnO₂ nanoparticles. The mixtures were prepared with the cement replacement by ZnO₂ nanoparticles from 1 to 5 weight percent and 1 weight percent polycarboxylate admixture.

The water to binder ratio for all mixtures was set at 0.40. The binder content of all mixtures was 450 kg.m⁻³. The proportions of the mixtures are presented in Table 4.

2.3. Test procedure

For NVC series concrete, Cylinders with the diameter of 150 mm and the height of 300 mm were cast and compacted in two layers on a vibrating table, where each layer was vibrated for 10 seconds. SCC series mixtures were prepared without subsequent vibration. The moulds were covered with polyethylene sheets and moistened for 24 hours. Then the specimens were demolded and cured in water and saturated limewater at a temperature of 20 °C prior to test days.

Splitting tensile tests were carried out according to the ASTM C 496^[29] standard. After the specified curing period was over (7, 28 and 90 days for NVC series and 2, 28 and 90 days for SCC series), the concrete cubes were subjected to splitting tensile test by using universal testing machine. The tests were carried out triplicately.

Water permeability tests are performed with several methods. In this work, water absorption has been selected to evaluate the water permeability of the specimens. Water absorption values samples were measured as per ASTM C 642^[30] after specified curing time in cold water. The tests were carried out triplicately.

3. Experimental Results

The splitting tensile strength results of the specimens are shown in Table 4. Table 4 shows that the splitting tensile strength increases with adding nano- ZnO₂ particles up to 1.0% in N-W series. It is shown that using 2.0% ZnO₂ nanoparticles decreases the splitting tensile strength to a value which is near to the control concrete. This may be due to the fact that the quantity of nano- ZnO₂ particles is higher than the amount required to combine with the liberated lime during the process of hydration thus leading to excess silica leaching out and causing a deficiency in strength as it replaces part of the cementitious material but does not contribute to strength³¹. Also, it may be due to the defects generated in dispersion of nanoparticles that causes weak zones. The high enhancement of splitting tensile strength in the N series blended concrete are due

Table 1. Chemical and physical properties of Portland cement (wt. (%)).

Material	SiO ₂	Al ₂ O ₃	Fe ₂ O ₃	CaO	MgO	SO ₃	Na ₂ O	K ₂ O	Loss on ignition
Cement	21.89	5.3	3.34	53.27	6.45	3.67	0.18	0.98	3.21

Specific gravity: 1.7 g.cm⁻³.

Table 2. The properties of nano- ZnO₂.

Diameter (nm)	Surface Volume ratio (m ² .g ⁻¹)	Density (g.cm ⁻³)	Purity (%)
15 ± 3	155 ± 12	<0.13	>99.9

Table 3. Physical and chemical characteristics of the polycarboxylate admixture.

Appearance	Yellow-brown liquid
% solid residue	Approximately 36%
pH	5.2-5.3
Specific gravity (kg.L ⁻¹)	Approximately 1.06
Rotational viscosity (MPa)	79.30
% C	52.25
ppm Na ⁺	9150
ppm K ⁺	158

to the rapid consuming of Ca(OH)₂ which was formed during hydration of Portland cement specially at early ages related to the high reactivity of nano- ZnO₂ particles. As a consequence, the hydration of cement is accelerated and larger volumes of reaction products are formed. Also nano- ZnO₂ particles recover the particle packing density of the blended cement, directing to a reduced volume of larger pores in the cement paste.

On the other hand, for the specimens saturated in limewater, the splitting tensile strength increases by adding up to 2.0 weight percent ZnO₂ nanoparticles. Lime reacts with water and produces Ca(OH)₂ which needs to form strengthening gel. When ZnO₂ nanoparticles react with Ca(OH)₂ produced from saturated limewater, the content of strengthening gel is increased because of high free energy of nanoparticles which reduces significantly when reacts by Ca(OH)₂. Table 4 also shows the water absorption in C0 and N series concrete. The results indicate similar results to splitting tensile strength.

Table 4 also shows the splitting tensile strength of C0-SCC and N-SCC specimens at 2, 7 and 28 days of curing. The results show that the splitting tensile strength increases by adding ZnO₂ nanoparticles up to 4.0 weight percent replacements (N4-SCC series) and then it decreases, although adding 5.0 percent ZnO₂ nanoparticles produces specimens with much higher splitting tensile strength with respect to C0-SCC and N-SCC specimens with 1.0, 2.0 and 3.0 weight percent ZnO₂ nanoparticles.

To show that nanoparticles are capable to improve the mechanical properties of concrete specimens significantly, the compressive strength of the specimens has been illustrated in Table 4. It is obvious that nanoparticles have a key role on increasing the compressive strength of the specimens.

Table 4 also shows the water absorption in C0-SCC and N-SCC series concrete. The results indicate improvement by adding nanoparticles similar to splitting tensile strength.

The mechanism that the nanoparticles improve the strength and resistance to water permeability of concrete specimens can be interpreted as follows³²: Suppose that

nanoparticles are uniformly dispersed in concrete and each particle is contained in a cube pattern, therefore the distance between nanoparticles can be determined. After the hydration begins, hydrate products diffuse and envelop nanoparticles as kernel³². If the content of nanoparticles and the distance between them are appropriate, the crystallization will be controlled to be a suitable state through restricting the growth of Ca(OH)₂ crystal by nanoparticles. Moreover, the nanoparticles located in cement paste as kernel can further promote cement hydration due to their high activity. This makes the cement matrix more homogeneous and compact. Consequently, the strength and resistance to water permeability of concrete is improved evidently such as the concrete containing nano- ZnO₂ in the amount of 1% by weight of binder³².

With increasing the content of ZnO₂ nanoparticles more than a specific weight percent (based on the concrete type), the improvement on the strength and resistance to water permeability of concrete is weakened. This can be attributed to that the distance between nanoparticles decreases with increasing content of nanoparticles, and Ca(OH)₂ crystal cannot grow up enough due to limited space and the crystal quantity is decreased, which leads to the ratio of crystal to strengthening gel small and the shrinkage and creep of cement matrix increased³³, thus the strength and resistance to water permeability of cement matrix is looser relatively.

On the whole, the addition of nanoparticles improves the strength and resistance to water permeability of concrete. On the one hand, nanoparticles can act as a filler to enhance the density of concrete, which leads to the porosity of concrete reduced significantly. On the other hand, nanoparticles can not only act as an activator to accelerate cement hydration due to their high activity, but also act as a kernel in cement paste which makes the size of Ca(OH)₂ crystal smaller and the tropism more stochastic.

4. Artificial Neural Networks

ANNs were developed to model the human brain³⁴. Even an ANN fairly simple and small in size when compared to the human brain, has some powerful characteristics in knowledge and information processing because of its similarity to the human brain. Therefore, an ANN can be a powerful tool for engineering applications³⁵. McCulloch and Pitts³⁶ defined artificial neurons for the first time and developed a neuron model as in Figure 1. McCulloch and Pitts' network³⁶ formed the basis for almost all later neural network models. Afterwards, Rosenblatt³⁷ devised a machine called the perceptron that operated much in the same way

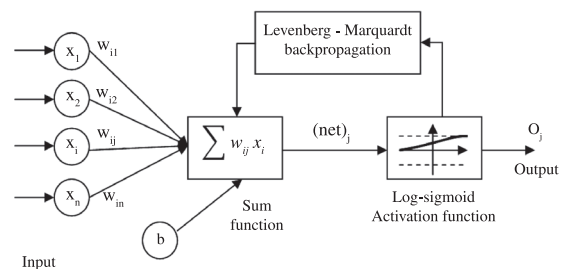
**Figure 1.** Architecture of applied neural network³⁶.

Table 4. Average splitting tensile strength and water absorption of different mixture proportion of concrete specimens.

Sample designation	ZnO ₂ nanoparticles (%)	PC content (%)	Quantities (kg.m ⁻³)		Average splitting tensile strength (MPa)						Average compressive strength (MPa)						Average water absorption (%)					
			Cement	ZnO ₂ nanoparticles	2 days	7 days	28 days	90 days	2 days	7 days	28 days	90 days	2 days	7 days	28 days	90 days	2 days	7 days	28 days	90 days		
					-	-	1.5	1.8	2.3	-	27.3	36.8	42.3	-	2.3	5.6	4.8					
C0-W	0	0	450.00	0.00	-	1.5	1.8	2.3	-	27.3	36.8	42.3	-	2.3	5.6	4.8						
N1-W	0.5	0	447.75	2.25	-	2.1	2.5	3.0	-	27.9	37.7	41.0	-	4.33	2.35	0.99						
N2-W	1.0	0	445.50	4.50	-	2.6	2.9	3.1	-	29.2	38.5	42.4	-	4.65	2.64	1.26						
N3-W	1.5	0	443.25	6.75	-	2.5	2.6	2.8	-	28.4	37.9	42.1	-	4.97	2.82	1.51						
N4-W	2.0	0	441.00	9.00	-	1.8	1.8	2.0	-	25.1	35.1	39.1	-	5.57	3.02	1.84						
C0-LW	0	0	450.00	0.00	-	1.3	1.5	1.9	-	27.0	35.4	39.8	-	4.32	5.71	4.92						
N1-LW	0.5	0	447.75	2.25	-	2.3	2.9	2.9	-	28.3	42.4	42.8	-	6.46	1.55	0.67						
N2-LW	1.0	0	445.50	4.50	-	3.1	3.2	3.3	-	31.3	44.5	45.0	-	6.91	1.67	0.92						
N3-LW	1.5	0	443.25	6.75	-	3.4	3.3	3.3	-	34.3	47.5	47.8	-	7.30	1.84	1.29						
N4-LW	2.0	0	441.00	9.00	-	3.7	3.5	3.5	-	37.1	49.7	49.7	-	7.48	2.00	1.53						
C0-SCC1	0	1.0	450.00	0.00	0.4	1.2	1.6	-	14.0	20.6	31.6	-	2.30	4.28	3.89	-						
N1-SCC1	1	1.0	445.50	4.50	0.7	1.1	1.4	-	13.4	21.6	31.6	-	4.29	2.2	2.02	-						
N2-SCC1	2	1.0	441.0	9.00	1.1	1.4	1.8	-	14.5	26.0	34.4	-	4.63	2.10	1.77	-						
N3-SCC1	3	1.0	437.5	13.50	1.4	1.8	2.2	-	16.0	29.2	40.0	-	5.01	1.96	1.47	-						
N4-SCC1	4	1.0	432.0	18.00	1.7	2.1	2.6	-	17.0	33.8	45.0	-	5.43	1.65	1.21	-						
N5-SCC1	5	1.0	427.5	22.50	1.5	1.9	2.3	-	18.2	31.8	43.8	-	5.20	1.76	1.35	-						

Water to binder [cement + nano- ZnO₂] ratio of 0.40. W denotes the specimens cured in water and LW denotes to those cured in saturated limewater.

as the human mind. Rosenblatt’s perceptrons³⁷ consist of “sensory” units connected to a single layer of McCulloch and Pitts³⁶ neurons. Rumelhardt et al.³⁸ derived a learning algorithm for perceptron networks with constituted hidden units. Their learning algorithm is called back-propagation and is now the most widely used learning algorithm. As a result of these studies, together with the developments in computer technology, using ANN has become more efficient after 1980^[39].

As it can be seen from Figure 1, an artificial neuron is composed of five main parts: inputs, weights, sum function, activation function and outputs. Inputs are information that enters the neuron from other neurons or from external world. Weights are values that express the outcome of an input set or another process element in the preceding layer on this process element. Sum function is a function that calculates the effect of inputs and weights completely on this process element. This function computes the net input that approaches to a neuron⁴⁰. The weighted sums of the input components (net)_j are calculated using Equation 1 as follows:

$$(net)_j = \sum_{i=1}^n W_{ij}x_i + b \tag{1}$$

where (net)_j is the weighted sum of the *j*th neuron in the input received from the preceding layer with *n* neurons, *W*_{ij} is the weight between the *j*th neuron in the previous layer, *x*_i is the output of the *i*th neuron in the previous layer³⁹. *b* is a fix value as internal addition and represents sum function. Activation function is a function that processes the net input obtained from sum function and determines the neuron output. In general for multilayer feed-forward models as the activation function sigmoid activation function is used. The output of the *j*th neuron (out)_j is computed using Equation 2 with a sigmoid activation function as follows⁴¹:

$$O_j = f(net)_j = \frac{1}{1 + e^{-\alpha(net)_j}} \tag{2}$$

where α is constant used to control the slope of the semi-linear region. The sigmoid nonlinearity activates in every layer except in the input layer³⁹. The sigmoid activation function represented by Equation 2 gives outputs in (0,1). If it desired, the outputs of this function can be adjusted to (-1,1) interval. As the sigmoid processor represents a continuous function it is particularly used in non-linear descriptions. Because its derivatives can be determined easily with regard to the parameters within (net)_j variable³⁹.

LMBP is often the fastest available back-propagation algorithm, and is highly recommended as a first-choice supervised algorithm, although it requires more memory than other algorithms. The standard LMBP training process can be described in the pseudocode of Figure 2^[42].

4.1. Neural network model structure and parameters

ANN model is carried out in this research has eight neurons in the input layer and one neurons in the output layer as demonstrated in Figure 3. The values for input layers were cement content (C), nanoparticle content (N),

```

1. Initialize the weights and parameter  $\mu$  ( $\mu = 0.01$  is appropriate).
2. Compute the sum of the squared errors over all inputs  $F(w)$ 
 $F(w) = e^T e$  (3)
Where  $w = [w_1, w_2, \dots, w_n]$  consists of all weights of the network,
 $e$  is the error vector comprising the error for all the training
examples.
3. Solve (5) to obtain the increment of weights  $w$ 
 $w = [J^T J + \mu I]^{-1} J^T e$  (4)
Where  $J$  is the Jacobian matrix,  $\mu$  is the learning rate which is to
be updated using the  $\beta$  depending on the outcome. In particular,
 $\mu$  is multiplied by decay rate  $\beta$  ( $0 < \beta < 1$ ).
4. Using  $w + w$  as the trial  $w$ , and judge
IF trial  $F(w) < F(w)$  in step 2 THEN
 $W = w + w$ 
 $\mu = \mu \cdot \beta$  ( $\beta = 0.1$ )
    go back to step 2
ELSE
 $\mu = \mu / \beta$ 
    go back to step 4
END IF
    
```

Figure 2. Pseudo-code for LMBP algorithm⁴²

aggregate type (AG), water content (W), the amount of superplasticizer (S), the type of curing medium (CM), Age of curing (AC) and number of testing try (NT). The values for output layer were splitting tensile strength (*f_s*) data in one set and water absorption (*f_w*) in the other set. Two hidden layer with ten and eight neurons were used in the architecture of multilayer neural network because of its minimum absolute percentage error values for training and testing sets. The neurons of neighboring layers are completely interconnected by weights. Finally, the output layer neurons produce the network prediction as a result.

In this study, the back-propagation training algorithm has been utilized in feed-forward two hidden layers. Back-propagation algorithm, as one of the most well-known training algorithms for the multilayer perceptron, is a gradient descent technique to minimize the error for a particular training pattern in which it adjust the weights by a small amount at a time⁴². The non-linear sigmoid activation function was used in the hidden layer and the neuron outputs at the output layer. Momentum rate and learning rate values were determined and the model was trained through iterations. The trained model was only tested with the input values and the predicted results were close to experiment results. The values of parameters used in neural network model are given in Table 5.

To make a decision on the completion of the training processes, two termination states are declared: state 1 (ANN-I model) means that the training of neural network was ended when the maximum epoch of process reached (1000) while state 2 (ANN-II model) means the training ended when minimum error norm of network gained.

5. Genetic Programming

Genetic programming (GP) proposed by Koza⁴³ is an extension to Genetic Algorithms (GA). Koza⁴³ defines GP as a domain independent problem-solving approach in which computer programs are evolved to solve, or approximately solve, problems based on the Darwinian

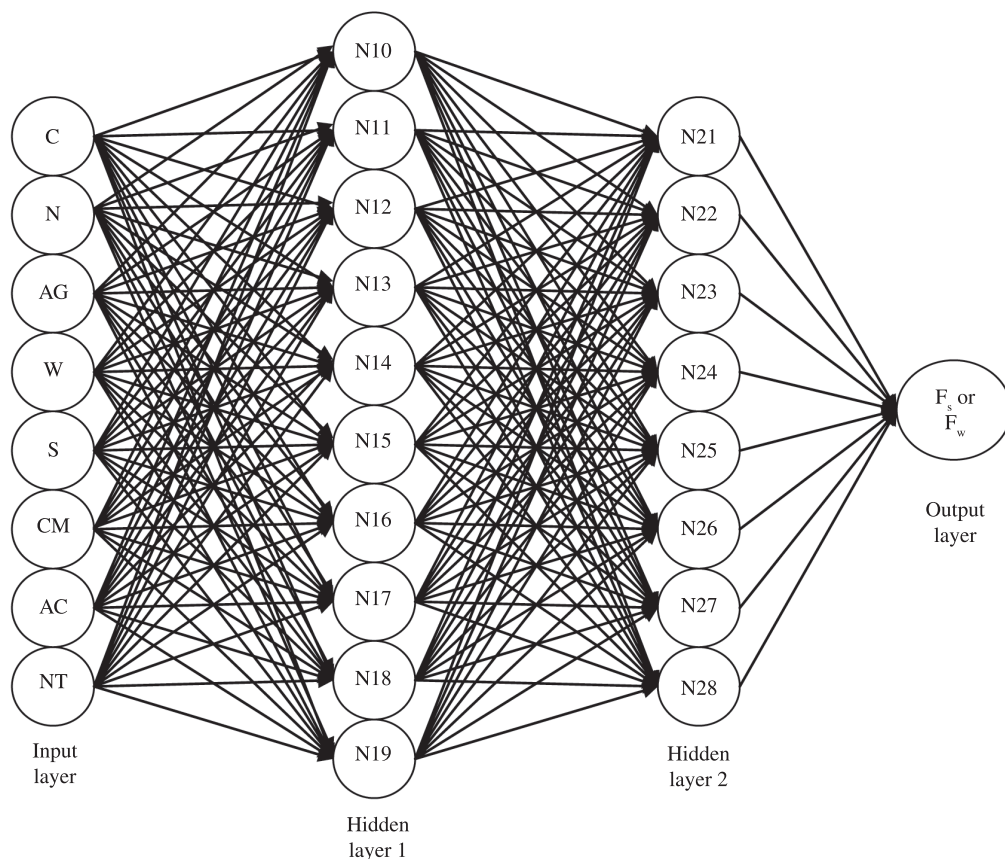


Figure 3. The system used in the ANN model.

Table 5. The values of parameters used in neural network model.

Parameters	ANN
Number of input layer units	8
Number of hidden layer	2
Number of first hidden layer units	10
Number of second hidden layer units	8
Number of output layer units	1
Momentum rate	0.88
Learning rate	0.70
Error after learning	0.000050
Learning cycle	30.000

principle of reproduction and survival of the fittest and analogs of naturally occurring genetic operations such as crossover and mutation. GP reproduces computer programs to solve problems by executing the steps in Figure 4. This figure is a flowchart showing the executional steps of a run of GP. The flowchart demonstrates the genetic operations in addition to the architecture changing operations. Also, this flowchart demonstrates a two offspring version of the crossover operation.

Gene expression programming (GEP) software which is used in this study is an extension to GEP that evolves

computer programs of different sizes and shapes encoded in linear chromosomes of fixed length. The chromosomes are composed of multiple genes, each gene encoding a smaller sub-program. Furthermore, the structural and functional organization of the linear chromosomes allows the unconstrained operation of important genetic operators such as mutation, transposition, and recombination⁴⁴⁻⁴⁶. The two main parameters GEP are the chromosomes and expression trees (ETs)⁴⁴⁻⁴⁶. Two languages are utilized in GEP: the language of the genes and the language of ETs. A significant advantage of GEP is that it enables to infer exactly the phenotype given the sequence of a gene, and vice versa which is termed as Karva language.

For each problem, the type of linking function, as well as the number of genes and the length of each gene, are a priori chosen for each problem. While attempting to solve a problem, one can always start by using a single-gene chromosome and then proceed by increasing the length of the head. If it becomes very large, one can increase the number of genes and obviously choose a function to link the sub-ETs. One can start with addition for algebraic expressions or for Boolean expressions, but in some cases another linking function might be more appropriate (like multiplication or IF, for instance). The idea, of course, is to find a good solution, and GEP provides the means of finding one very efficiently⁴⁴.

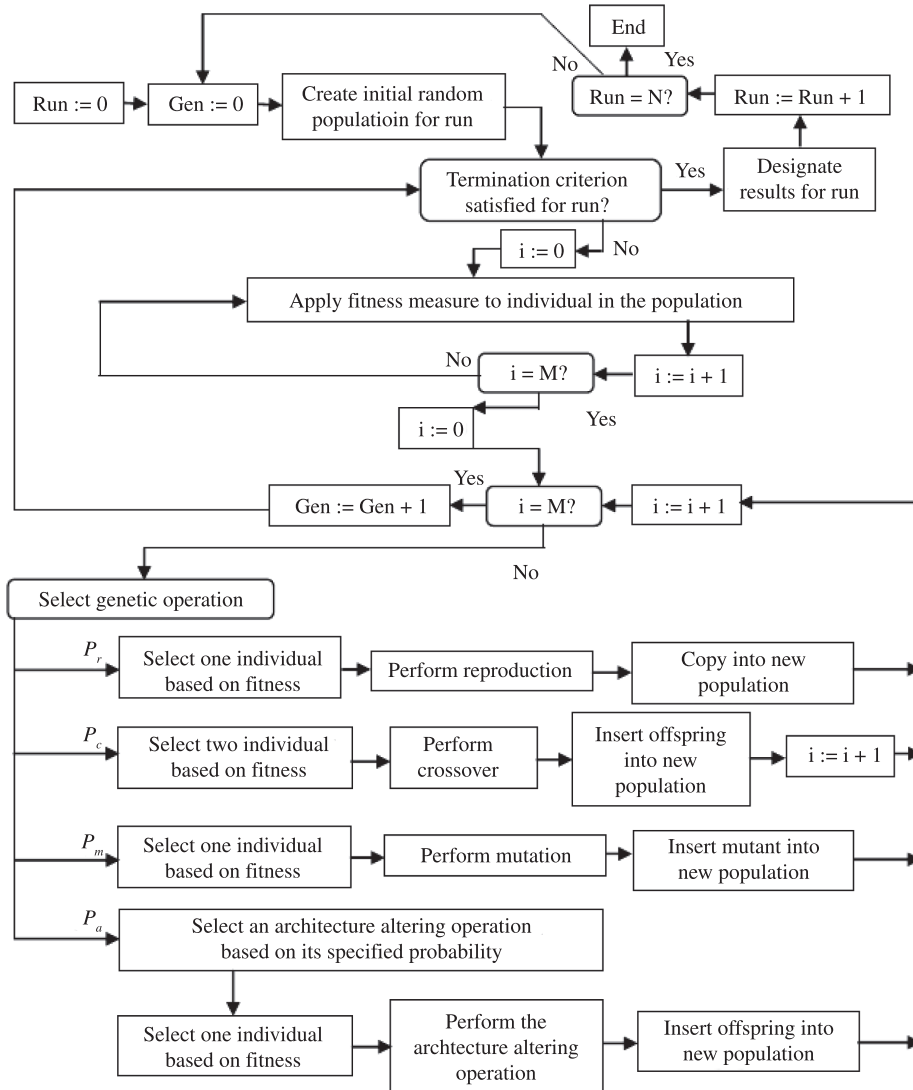


Figure 4. Genetic programming flowchart⁴³.

5.1. Genetic expression programming structure and parameters

In this study, as seen in Figures 5-8, the expression trees of two different GEP approach models namely GEP-I and GEP-II were constructed for splitting tensile strength and water absorption. d0, d1, d2, d3, d4, d5 d6 and d7 in Figures 5-8 represent C, N, AG, W, S, CM, AC and NT, respectively. In the GEP-I and GEP-II, as the number of genes used 3 and 4 genes (Sub-ETs), and as linking function used addition and multiplication, respectively. In training and testing of the GEP-I and GEP-II approach models constituted with two different Sub-ETs and linking function C, N, AG, W, S, CM, AC and NT as input data and f_s and f_w as independent output data. Among 144 experimental sets, 117 sets were randomly chosen as a training set for the GEP-I and GEPII modeling and the remaining 27 sets were used as testing the generalization capacity of the proposed models.

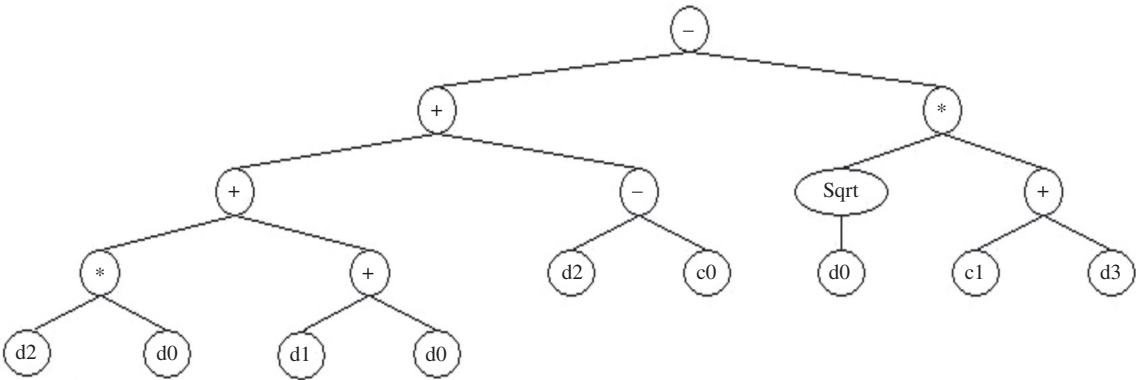
For this problem, firstly, the fitness, f_i , of an individual program, i , is measured by:

$$f_i = \sum_{j=1}^{C_i} (M - |C_{(ij)} - T_j|) \quad (5)$$

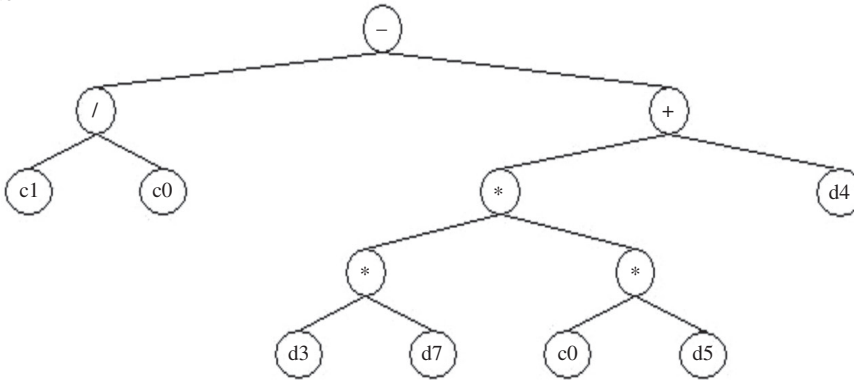
where M is the range of selection, $C_{(ij)}$ is the value returned by the individual chromosome i for fitness case j (out of C_i fitness cases) and T_j is the target value for fitness case j . If $|C_{(ij)} - T_j|$ (the precision) is less than or equal to 0.01, then the precision is equal to zero, and $f_i = f_{\max} = C_i M$. In this case, $M = 100$ was used, therefore, $f_{\max} = 1000$. The advantage of this kind of fitness functions is that the system can find the optimal solution by itself^{44,47}.

Afterwards the set of terminals T and the set of functions F to create the chromosomes are preferred, namely, $T = \{C, N, AG, W, S, CM, AC, NT\}$ and four basic arithmetic operators $(+, -, *, /)$ and some basic mathematical functions (Sqrt, x^3) were used.

Sub-ET 1



Sub-ET 2



Sub-ET 3

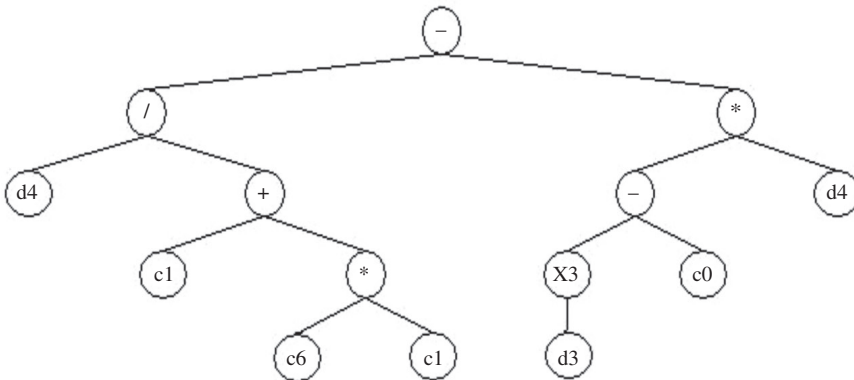


Figure 5. Expression tree with 3 gens for splitting tensile strength in GEP-I model. C0 = 12.25 and C1 = -3.37.

Another major step is to choose the chromosomal tree, i.e., the length of the head and the number of genes. The GEP-I and GEP-II approach models initially used single gene and two lengths of heads, and increased the number of genes and heads, one after another during each run, and monitored the training and testing sets performance of each model. In this study, for the GEP-I and GEP-II approach models observed the number of genes 3 and 4, and length of heads 10 and 12, respectively. In addition, for the GEP-I and GEP-II approach models determined the linking function multiplication and addition, respectively.

Finally, a combination of all genetic operators (mutation, transposition and crossover) was utilized as set of genetic operators. Parameters of the training of the GEP-I and GEP-II approach models are given in Table 6. For the

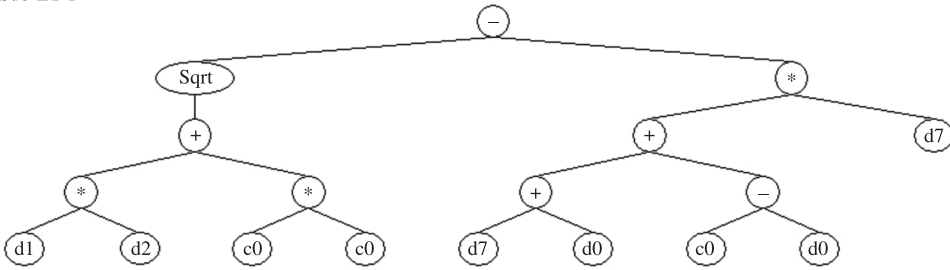
GEP-I and GEP-II approach models, chromosome 30 and 40 were observed to be the best of generation individuals predicting f_s and f_w . Explicit formulations based on the GEP-I and GEP-II approach models for f_s and f_w were obtained by:

$$f_s = f(C, N, AG, W, S, CM, AC, NT) \tag{6}$$

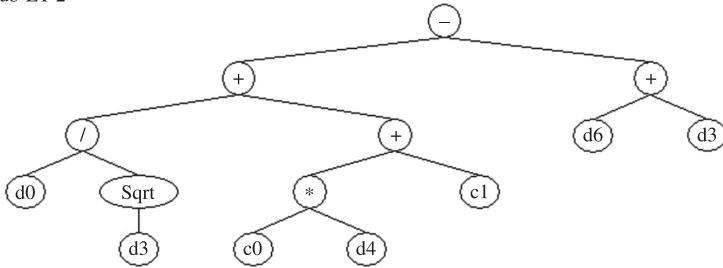
$$f_w = f(C, N, AG, W, S, CM, AC, NT) \tag{7}$$

Figures 5 and 6 show the expression trees with 3 and 4 gens respectively for splitting tensile strength prediction and Figures 7 and 8 show the expression trees with 3 and 4 gens respectively for water absorption prediction. The related formulations could be obtained by the procedure shown in Figure 9^[7].

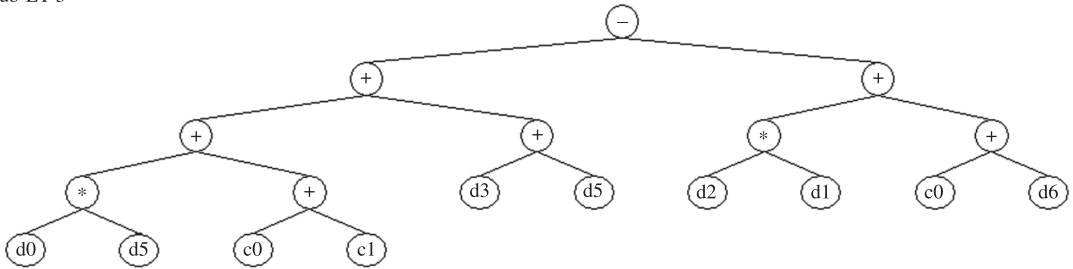
Sub-ET 1



Sub-ET 2



Sub-ET 3



Sub-ET 4

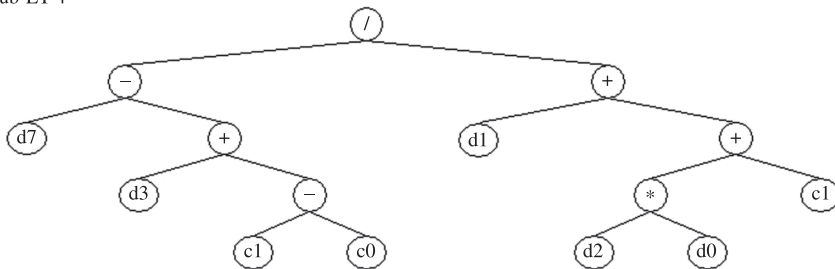
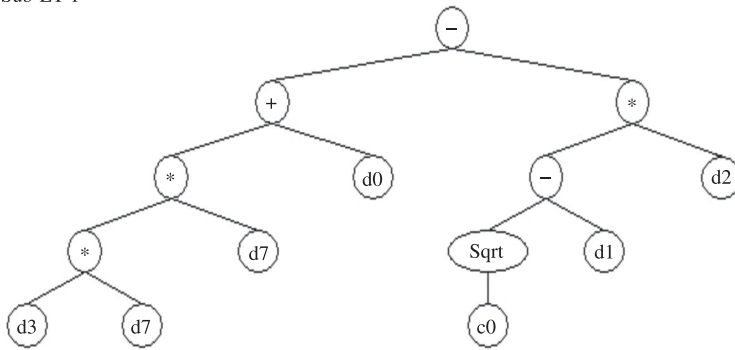


Figure 6. Expression tree with 4 gens for splitting tensile strength in GEP-II model. C0 = 18.95, c1 = 4.43.

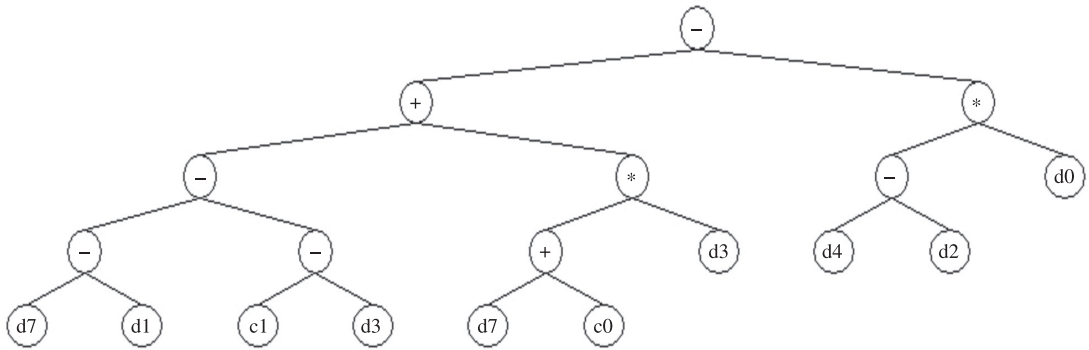
Table 6. Parameters of GEP approach models.

Parameter definition		GEP-I	GEP-II
P1	Function set	+, -, *, /, sqrt, x ³	+, -, *, /, sqrt, x ³
P2	Chromosomes	30	40
P3	Head size	12	14
P4	Number of genes	3	4
P5	Linking function	Addition	Multiplication
P6	Mutation rate	0.044	0.044
P7	Inversion rate	0.1	0.1
P8	One-point recombination rate	0.3	0.3
P9	Two-point recombination rate	0.3	0.3
P10	Gene recombination rate	0.1	0.1
P11	Gene transposition rate	0.1	0.1

Sub-ET 1



Sub-ET 2



Sub-ET 3

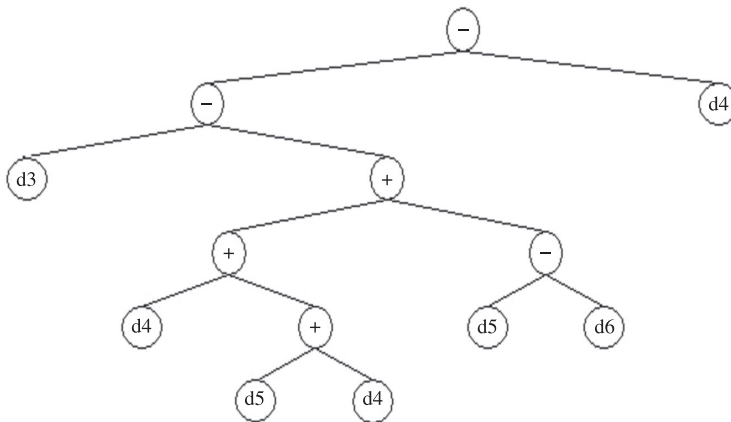


Figure 7. Expression tree with 3 gens for water absorption in GEP-I model. C0 = 3.56, c1 = -7.24.

6. Results

6.1. Artificial neural network

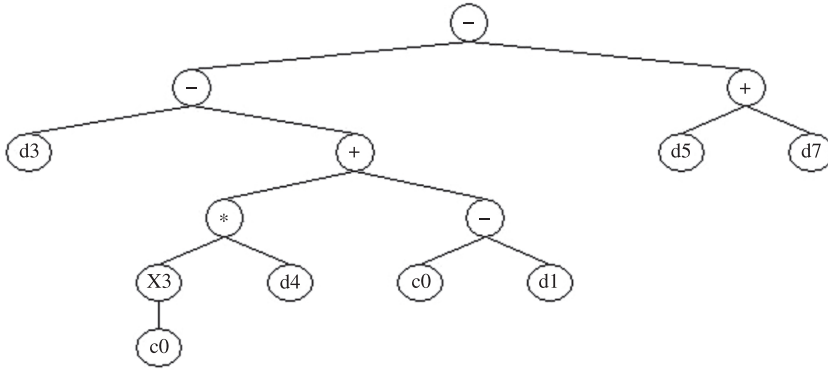
In this study, the error arose during the training and testing in ANN-I and ANN-II models can be expressed as absolute fraction of variance (R^2) which are calculated by Equation 8^[48]:

$$R^2 = 1 - \left(\frac{\sum_i (t_i - o_i)^2}{\sum_i (o_i)^2} \right) \quad (8)$$

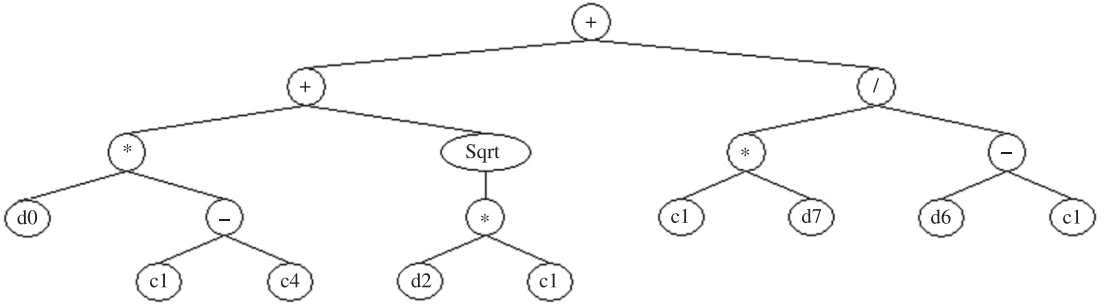
where t is the target value, o is the output value and p is the pattern.

All of the results obtained from experimental studies and predicted by using the training and testing results of ANN I and ANN II models, for f_s are given in Figures 10a, b, respectively and for f_w in Figures 11a, b, respectively. The linear least square fit line, its equation and the R^2 values were shown in these figures for the training and testing data. As it is visible in Figures 10 and 11 the values obtained from the training and testing in ANN-I and ANN-II models are very close to the experimental results. The result of testing phase in Figures 10 and 11 shows that the ANN-I and ANN-II models are capable of generalizing between input and output variables with reasonably good predictions.

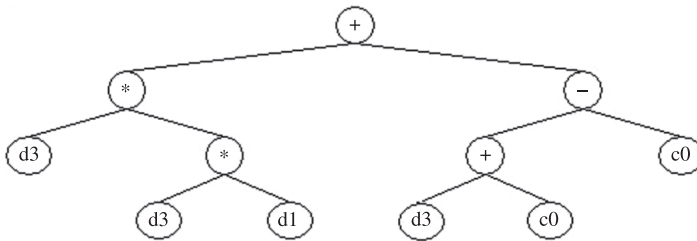
Sub-ET 1



Sub-ET 2



Sub-ET 3



Sub-ET 4

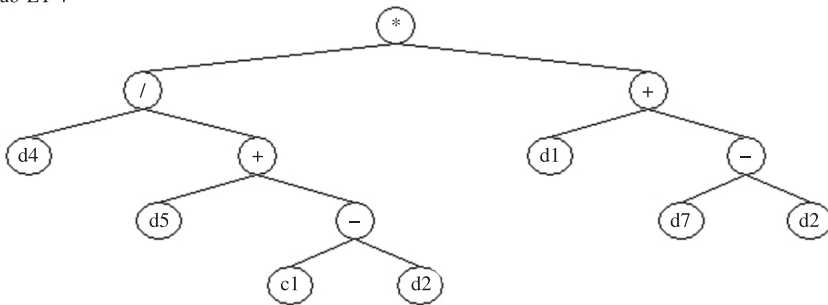


Figure 8. Expression tree with 4 gens for water absorption in GEP-II model. C0 = 7.54, c1 = 13.33.

The performance of the ANN-I and ANN-II models for f_s and f_w is shown in Figures 10 and 11, respectively. The best values of R^2 are 98.29 and 98.89% for training set in the ANN-II model, respectively for splitting tensile strength and water absorption. The minimum values of R^2 are 92.09 and

94.79% for testing set in the ANN-I model, respectively for splitting tensile strength and water absorption. All of R^2 values show that the proposed ANN-I and ANN-II models are suitable and can predict f_s and f_w values for every age very close to the experimental values.

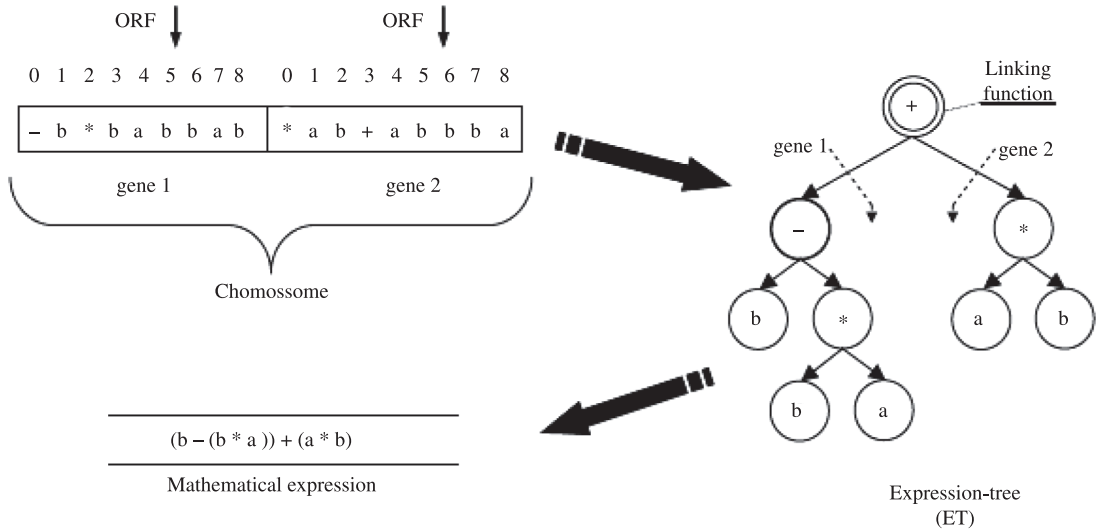


Figure 9. Chromosome with two genes and its decoding in GEP⁷.

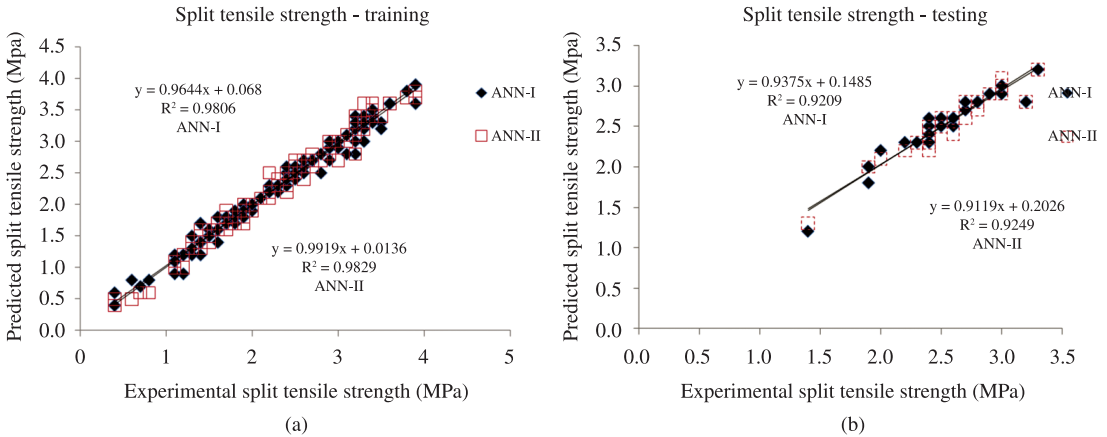


Figure 10. The correlation of the measured and predicted splitting tensile strengths in a) training and b) testing phase for ANN models.

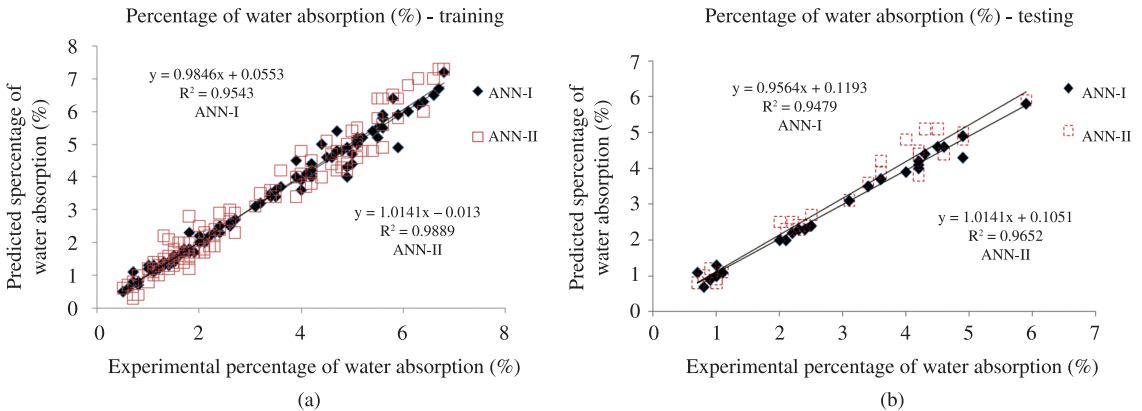


Figure 11. The correlation of the measured and predicted water absorption in a) training and b) testing phase for ANN models.

6.2. Genetic programming

Once again, in this study, the error arose during the training and testing in GEP-I and GEP-II models can be expressed as R² which are calculated by Equation 8. All of

the results obtained from experimental studies and predicted by using the training and testing results of GEP-I and GEP-II models, for f_s are given in Figures 12a, b, respectively and for F_w in Figures 13a, b, respectively. The linear least square fit line, its equation and the R² values were shown

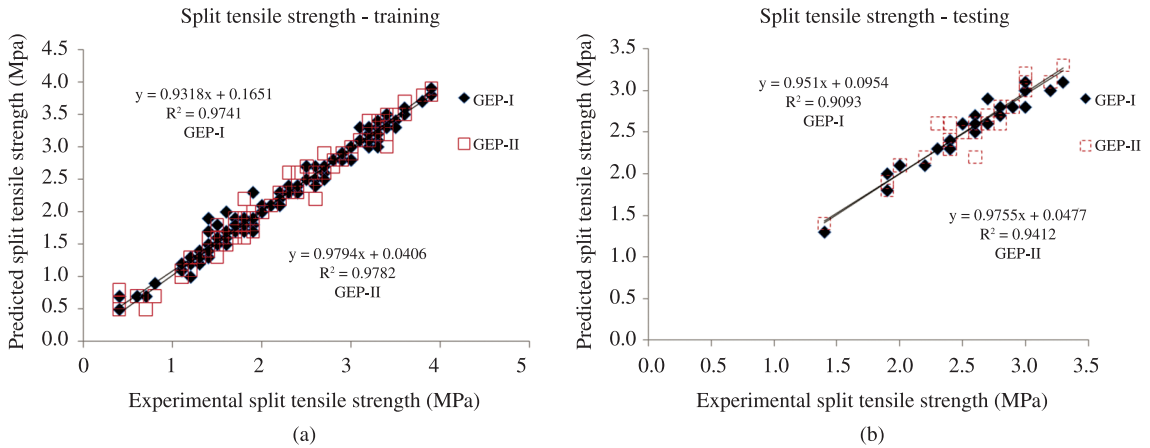


Figure 12. The correlation of the measured and predicted splitting tensile strengths in a) training and b) testing phase for GEP models.

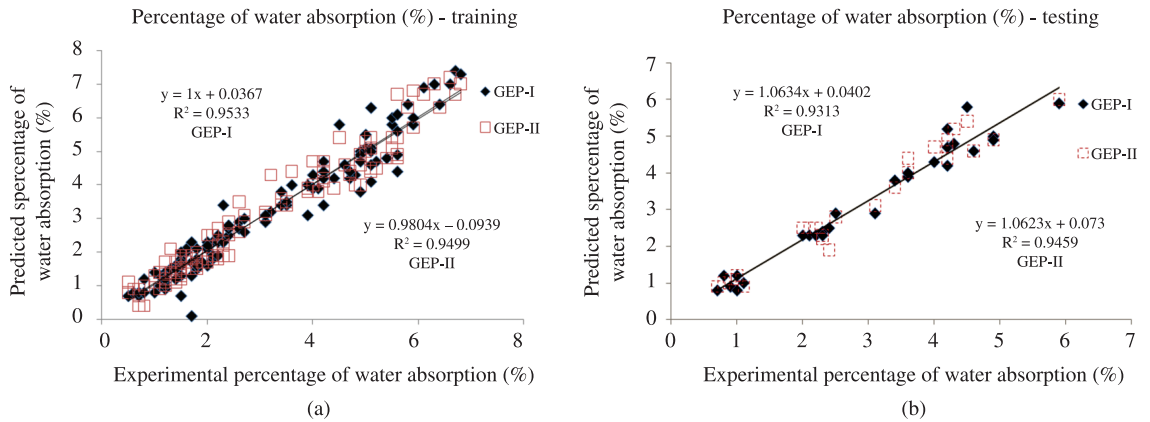


Figure 13. The correlation of the measured and predicted water absorption in a) training and b) testing phase for GEP models.

in these figures for the training and testing data. As it is visible in Figures 12 and 13 the values obtained from the training and testing in GEP-I and GEP-II models are very close to the experimental results. The result of testing phase in Figures 12 and 13 shows that the GEP-I and GEP-II models are capable of generalizing between input and output variables with reasonably good predictions.

The performance of the GEP-I and GEP-II models for f_s and f_w is shown in Figures 12 and 13, respectively. The best values of R^2 are 97.82 and 94.99% for training set in the GEP-II model, respectively for splitting tensile strength and water absorption. The minimum values of R^2 are 90.93 and 93.13% for testing set in the GEP-I model, respectively for splitting tensile strength and water absorption. All of the statistical values show that the proposed GEP-I and GEP-II models are suitable and can predict f_s and f_w values for every age very close to the experimental values.

7. Discussion

Artificial neural networks are capable of learning and generalizing from examples and experiences. This makes artificial neural networks a powerful tool for solving some of the complicated civil engineering problems. In this study, using these beneficial properties of artificial neural networks in order to predict the splitting tensile strength

and water absorption values of concretes containing ZnO_2 nanoparticles without attempting any experiments were developed two different multilayer artificial neural network architectures namely ANN-I and ANN-II. In two models developed in ANN method, a multilayered feed forward neural network with a back propagation algorithm was used. The models were trained with input and output data. Using only the input data in trained models the splitting tensile strength and water absorption values of concretes containing ZnO_2 nanoparticles were found. The splitting tensile strength and water absorption values predicted from training and testing, for ANN-I and ANN-II models, are very close to the experimental results. Furthermore, according to the splitting tensile strength and water absorption results predicted by using ANN-I and ANN-II models, the results of ANN-II model are closer to the experimental results. R^2 values that are calculated for comparing experimental results with ANN-I and ANN-II model results have shown this situation.

In addition, this study reports a new and efficient approach for the formulation of concrete containing ZnO_2 nanoparticles using GEP. Two different GEP-I and GEP-II approach models are proposed in order to predict splitting tensile strength and water absorption values of concrete containing ZnO_2 nanoparticles. The

proposed models are empirical and based on experimental results. The models developed in this study are used to be the number of genes 3 and 4, and the linking function addition and multiplication, respectively. All of the results obtained from the models show excellent agreement with experimental results. The statistical values of R² have shown this situation. Also, the proposed models are so simple that they can be used by anyone not necessarily familiar with GEP. Moreover, it is concluded that GEP is a good soft computing technique for use in concrete properties prediction. As a result, GEP may serve as a strong approach model and it may open a new area for the accurate and effective explicit formulation of many civil engineering problems.

From the predicted results for splitting tensile strength and water absorption, it is concluded that ANN models are more suitable for prediction the concrete properties. This conclusion is made on the R² values obtained from different applied models. However, application of GEP as a result of its simplicity is a relatively suitable approaches for prediction the concrete properties. The results show that both ANNs and GEP models have different R² values for splitting tensile strength and water absorption fitting in both training and testing data sets. This may be due to very close data in both splitting tensile strength and water absorption results. However, as mentioned, all of the predicted results fall in acceptable ranges.

References

- Ye G, Lura P and Van Breugel K. Modelling of water permeability in cementitious materials. *Materials and Structures*. 2006; 39: 877-885. <http://dx.doi.org/10.1617/s11527-006-9138-4>
- Hong-Guang N and Ji-Zong W. Prediction of compressive strength of concrete by neural networks. *Cement and Concrete Research*. 2000; 30(8):1245-50. [http://dx.doi.org/10.1016/S0008-8846\(00\)00345-8](http://dx.doi.org/10.1016/S0008-8846(00)00345-8)
- Pala M, Ozbay O, Oztas A and Yuce MI. Appraisal of long-term effects of fly ash and silica fume on compressive strength of concrete by neural networks. *Construction and Building Materials*. 2005; 21(2):384-94. <http://dx.doi.org/10.1016/j.conbuildmat.2005.08.009>
- Akkurt S, Tayfur G and Can S. Fuzzy logic model for prediction of cement compressive strength. *Cement and Concrete Research*. 2004; 34(8):1429-33. <http://dx.doi.org/10.1016/j.cemconres.2004.01.020>
- Baykasoğlu A, Dereli T and Tanış S. Prediction of cement strength using soft computing techniques. *Cement and Concrete Research*. 2004; 34(11):2083-90. <http://dx.doi.org/10.1016/j.cemconres.2004.03.028>
- Akkurt S, Ozdemir S, Tayfur G and Akyol B. The use of GA-ANNs in the modelling of compressive strength of cement mortar. *Cement and Concrete Research*. 2003; 33(7):973-9. [http://dx.doi.org/10.1016/S0008-8846\(03\)00006-1](http://dx.doi.org/10.1016/S0008-8846(03)00006-1)
- Cevik A and Sonebi M. Genetic programming based formulation for fresh and hardened properties of self-compacting concrete containing pulverised fuel ash. *Construction and Building Materials*. 2009; 23(7):2614-22. <http://dx.doi.org/10.1016/j.conbuildmat.2009.02.012>
- Cevik A and Sonebi M. Modelling the performance of self-compacting SIFCON of cement slurries using genetic programming technique. *Computers and Concrete*. 2008; 5(5):475-91.
- Nazari A and Riahi S. Microstructural, thermal, physical and mechanical behavior of the self compacting concrete containing SiO₂ nanoparticles. *Materials Science and Engineering: A*. 2010; 527:7663-7672. <http://dx.doi.org/10.1016/j.msea.2010.08.095>
- Nazari A and Riahi S. The effect of TiO₂ nanoparticles on water permeability and thermal and mechanical properties of high strength self-compacting concrete. *Materials Science and Engineering: A*. 2010; 528(2):756-763. <http://dx.doi.org/10.1016/j.msea.2010.09.074>
- Nazari A. The effects of curing medium on flexural strength and water permeability of concrete incorporating TiO₂ nanoparticles. *Materials and Structures*. 2011; 44(4): 773-786. <http://dx.doi.org/10.1617/s11527-010-9664-y>
- Nazari A and Riahi S. The effects of zinc dioxide nanoparticles on flexural strength of self-compacting concrete. *Composites Part B: Engineering*. 2011; 42:167-175. <http://dx.doi.org/10.1016/j.compositesb.2010.09.001>
- Nazari A and Riahi S. Computer-aided prediction of physical and mechanical properties of high strength cementitious composite containing Cr₂O₃ nanoparticles. *Nano*. 2010; 5(5):301-318. <http://dx.doi.org/10.1142/S1793292010002219>
- Nazari A and Riahi S. The effects of SiO₂ nanoparticles on physical and mechanical properties of high strength self compacting concrete. *Composites Part B: Engineering*. 2011; 42:570-578. <http://dx.doi.org/10.1016/j.compositesb.2010.09.025>
- Nazari A and Riahi S. Improvement compressive strength of cementitious composites in different curing media by Al₂O₃ nanoparticles. *Materials Science and Engineering:*

- A. 2011; 528:1183-1191. <http://dx.doi.org/10.1016/j.msea.2010.09.098>
16. Nazari A and Riahi S. The effects of Cr₂O₃ nanoparticles on strength assessments and water permeability of concrete in different curing media. *Materials Science and Engineering: A*. 2011; 528:1173-1182. <http://dx.doi.org/10.1016/j.msea.2010.09.099>
 17. Nazari A and Riahi S. ZrO₂ nanoparticles effects on split tensile strength of self compacting concrete. *Materials Research*. 2010; 13(4):485-495. <http://dx.doi.org/10.1590/S1516-14392010000400011>
 18. Nazari A and Riahi S. The effects of ZrO₂ nanoparticles on physical and mechanical properties of high strength self compacting concrete. *Materials Research*. 2010; 13(4): 551-556. <http://dx.doi.org/10.1590/S1516-14392010000400019>
 19. Nazari A and Riahi S. The effects of ZnO nanoparticles on strength assessments and water permeability of concrete in different curing media. *Materials Research*. 2011; 14(2):178-188. <http://dx.doi.org/10.1590/S1516-14392011005000030>
 20. Nazari A and Riahi S. Al₂O₃ nanoparticles in concrete and different curing media. *Energy and Buildings*. 2011; 43:1480-1488. <http://dx.doi.org/10.1016/j.enbuild.2011.02.018>
 21. Riahi S and Nazari A. Physical, mechanical and thermal properties of concrete in different curing media containing ZnO₂ nanoparticles. *Energy and Buildings*. 2011; 43:1977-1984. <http://dx.doi.org/10.1016/j.enbuild.2011.04.009>
 22. Nazari A and Riahi S. Effects of CuO Nanoparticles on Microstructure, Physical, Mechanical and Thermal Properties of Self-Compacting Cementitious Composites. *Journal of Materials Science and Technology*. 2011; 27(1):81-92. [http://dx.doi.org/10.1016/S1005-0302\(11\)60030-3](http://dx.doi.org/10.1016/S1005-0302(11)60030-3)
 23. Nazari A and Riahi S. Splitting tensile strength of concrete using ground granulated blast furnace slag and SiO₂ nanoparticles as binder. *Energy and Buildings*. 2011; 43:864-872. <http://dx.doi.org/10.1016/j.enbuild.2010.12.006>
 24. Nazari A and Riahi S. TiO₂ nanoparticles effects on physical, thermal and mechanical properties of self compacting concrete with ground granulated blast furnace slag as binder. *Energy and Buildings*. 2011; 43:995-1002. <http://dx.doi.org/10.1016/j.enbuild.2010.12.025>
 25. Nazari A and Riahi S. Optimization ZnO₂ nanoparticles content in binary blended concrete to enhance high strength concrete. *International Journal of Materials Research*. 2011; 102(4):457-463. <http://dx.doi.org/10.3139/146.110497>
 26. Nazari A and Riahi S. CuO nanoparticles' effects on compressive strength of self compacting concrete. *Sadhana*. 2011; 36(3):371-391. <http://dx.doi.org/10.1007/s12046-011-0023-7>
 27. Nazari A and Riahi S. Physical and mechanical behavior of high strength self compacting concrete containing ZrO₂ nanoparticles. *International Journal of Materials Research*. 2011; 102(5):560-571. <http://dx.doi.org/10.3139/146.110509>
 28. American Society for Testing and Materials – ASTM. *ASTM C150*: Standard Specification for Portland Cement. Philadelphia: ASTM; 2001.
 29. American Society for Testing and Materials – ASTM. *ASTM C39*: Standard Test Method for Compressive Strength of Cylindrical Concrete Specimens. Philadelphia: ASTM; 2001.
 30. American Society for Testing and Materials – ASTM. *ASTM C642*: Standard Test Method for Density, Absorption, and Voids in Hardened Concrete. Philadelphia: ASTM; 2001.
 31. Shih JY, Chang TP and Hsiao TC. Effect of nanosilica on characterization of Portland cement composite. *Cement and Concrete Research*. 2006; 36:697-706.
 32. Li H, Zhang M and Ou J. Flexural fatigue performance of concrete containing nanoparticles for pavement. *International Journal of Fatigue*. 2007; 29:1292-1301. <http://dx.doi.org/10.1016/j.ijfatigue.2006.10.004>
 33. Ye Q. The study and development of the nano-composite cement structure materials. *New Building Materials*. 2001; (1):4-6.
 34. Mukherjee A and Biswas SN. Artificial neural networks in prediction of mechanical behavior of concrete at high temperature. *Nuclear Engineering and Design*. 1997; 178(1):1-11. [http://dx.doi.org/10.1016/S0029-5493\(97\)00152-0](http://dx.doi.org/10.1016/S0029-5493(97)00152-0)
 35. Ince R. Prediction of fracture parameters of concrete by artificial neural networks. *Engineering Fracture Mechanics*. 2004; 71(15):2143-59. <http://dx.doi.org/10.1016/j.engfracmech.2003.12.004>
 36. McCulloch WS and Pitts W. A logical calculus of the ideas immanent in neural nets. *Bulletin of Mathematical Biophysics*. 1943; 5:115-37. <http://dx.doi.org/10.1007/BF02478259>
 37. Rosenblatt F. *Principles of neuro dynamics*: perceptrons and the theory of brain mechanisms. Washington: Spartan Books; 1962.
 38. Rumelhart DE, Hinton GE and William RJ. Learning internal representation by error propagation. In: Rumelhart DE and McClelland JL, editors. *Proceeding parallel distributed processing foundation*. Cambridge: MIT Press; 1986. vol. 1.
 39. Liu SW, Huang JH, Sung JC and Lee CC. Detection of cracks using neural networks and computational mechanics. *Computer Methods in Applied Mechanics and Engineering*. 2002; 191(25-26):2831-45. [http://dx.doi.org/10.1016/S0045-7825\(02\)00221-9](http://dx.doi.org/10.1016/S0045-7825(02)00221-9)
 40. Anderson JA. Cognitive and psychological computation with neural models. *IEEE Systems, Man, and Cybernetics*. 1983; 5:799-814.
 41. Hopfield JJ. Neural networks and physical systems with emergent collective computational abilities. *Proceedings of the National Academy of Sciences*. 1982; 79:2554-8. <http://dx.doi.org/10.1073/pnas.79.8.2554>
 42. Suratgar AA, Tavakoli MB and Hoseinabadi A. Modified Levenberg-Marquardt method for neural networks training. *World Academy of Science, Engineering and Technology*. 2005; 6:46-8.
 43. Koza JR. *Genetic programming*: on the programming of computers by means of natural selection. Cambridge: MIT Press; 1992.
 44. Ferreira C. Gene expression programming in problem solving. In: Invited tutorial of the 6th online world conference on soft computing in industrial applications; 2001.
 45. Ferreira C. Gene expression programming: a new adaptive algorithm for solving problems. *Complex Systems*. 2001; 13(2):87-129.
 46. Ferreira C. *Gene expression programming*: mathematical modeling by an artificial intelligence. Springer-Verlag; 2002.
 47. Çiftci ON, Fadiloğlu S, Goğuş F and Guven A. Genetic programming approach to predict a model acidolysis system. *Engineering Applications of Artificial Intelligence*. 2009; 22(4-5):759-66. <http://dx.doi.org/10.1016/j.engappai.2009.01.010>
 48. Topçu IB and Sarıdemir M. Prediction of compressive strength of concrete containing fly ash using artificial neural network and fuzzy logic. *Computational Materials Science*. 2008; 41(3):305-11. <http://dx.doi.org/10.1016/j.commatsci.2007.04.009>